

# Grazing Angle Attenuated Total Reflection Spectroscopy: Fields at the Interface and Source of the Enhancement

MILAN MILOSEVIC,\* VIOLET MILOSEVIC, and S. L. BERETS

*MeV Photonics, Westport, Connecticut 06880; and Harrick Scientific Products, Pleasantville, New York 10570*

With the tremendous growth in the semiconductor and coatings industries, spectroscopic methods of examining extremely thin films on high refractive index substrates have become increasingly important. One infrared method for analyzing monolayers on substrates such as silicon and gold that has recently gained popularity is ‘grazing’ or high angle of incidence attenuated total reflection (ATR) spectroscopy. This paper investigates the directional electric field strengths and the extraordinary sensitivity achieved by using the grazing angle ATR method for analyzing monolayers on silicon substrates.

Index Headings: Attenuated total reflection spectroscopy; ATR spectroscopy; Monolayers; Silicon substrate; Metal substrate; Electric field strength; Sensitivity enhancement.

## INTRODUCTION

Monolayers and extremely thin films on metal and silicon substrates are of great interest to various branches of science and technology, including the semiconductor and electronics industries. Thus, it is important to be able to spectroscopically study these films in order to gain insight into their structure, thickness, and molecular orientation. However, traditional spectroscopic methods of investigating thin films generally result in very weak bands. If the film is deposited on an infrared transparent substrate, such as Si, for analysis by transmission, the resulting infrared band intensity depends on film thickness in accordance with Lambert’s law. Monolayers are extremely thin and their absorption bands are close to the detection limit. Consider, for example, a typical vegetable oil that has an absorption index for the carbonyl band at  $1750\text{ cm}^{-1}$  of  $\kappa = 0.08$ . For a  $50\text{ \AA}$  thick coating, the absorbance measured would be approximately 0.00088 absorbance units, essentially at the detection limit. If the film is deposited on an opaque substrate, like a metal, only reflectance techniques can be used for analysis. Monolayers on metal substrates can be examined by grazing angle specular reflection using  $p$ -polarized light, although the peaks are close to the detection limit with this method and various signal enhancement techniques, such as polarization modulation, generally have to be employed. Silicon substrates might seem to be amenable to grazing angle reflection spectroscopy due to their high refractive index and resulting high reflectance from the surface. However, the reflectance from silicon for  $p$ -polarized light at grazing angle is low because grazing angle is near its Brewster’s angle. Thus, very little light is reflected from the surface at grazing angle. In addition, the spectral interpretation of the resulting spectra is not straightforward because the resulting absorption bands associated with the film can be inverted and distorted. Thus, grazing angle spectroscopy does not lend itself to the analysis of thin films on silicon substrates, except possibly in some special cases.

Another technique, grazing angle attenuated total reflection (GAATR), has recently become popular for analyzing thin films on metal or silicon substrates using variable angle ATR accessories such as the Harrick Seagull or dedicated accessories like the Harrick GATR. Although the beginnings of this technique date to the early days of ATR<sup>1</sup> and were subsequently utilized by other researchers,<sup>2</sup> GAATR has remained largely unknown until recent work<sup>3–9</sup> showed that GAATR exhibits a sensitivity amplification to thin films not only on silicon substrates but on metal substrates as well. Interestingly, this enhancement is not some new and unexplained phenomenon. The expression for reflectance based on Fresnel formulae clearly indicates the enhancement, as identified in Ref. 2 within the simplified expression for reflectance derived in Ref. 1.

The underlying phenomenon that causes the enhancement originates from the electric field strength of the electromagnetic wave within the film. It is particularly important to understand the strength of the different field components, as they can only be absorbed by an electric dipole from a molecular bond oscillating in the direction of that component. This paper discusses the theoretical basis for the extraordinary sensitivity achieved by the grazing angle ATR method by examining the electric field components within a typical very thin film.

## THEORY

**Thin Film Reflectance Formula.** Consider the case where light interacts with a three-layer system as shown in Fig. 1. The wave of amplitude  $A_{\text{in}}$  is incident from medium 1 with refractive index  $n_1$ . For simplicity, in Fig. 1 we used generic amplitude  $A$  rather than a specific field component of a propagating wave. To substitute any specific field component for  $A$ , attention has to be paid to the field orientation as in Fig. 2.

The film (medium 2) is characterized by a complex refractive index  $n_2$  and the substrate (medium 3) by the refractive index  $n_3$ . Because of the presence of the second interface, the refracted wave  $A_+$  reflects from the second interface, generating a returning wave  $A_-$ . This returning wave partially reflects on the first interface, thus adding to  $A_+$ , and partially transmits, contributing to the reflected wave  $A_r$ . The internally reflecting wave loses energy at every reflection and hence contributes smaller and smaller components to  $A_r$  with each subsequent reflection from the first interface.

The expression for the amplitude reflectance coefficient of a system of two parallel interfaces with a distance  $d$  separating three media optically characterized by the refractive indices  $n_1$ ,  $n_2$ , and  $n_3$  is:<sup>10</sup>

$$\rho^\sigma = \frac{r_{12}^\sigma + r_{23}^\sigma e^{4\pi i n_2 d \sqrt{n_2^2 - n_1^2 \sin^2 \theta}}}{1 + r_{12}^\sigma r_{23}^\sigma e^{4\pi i n_2 d \sqrt{n_2^2 - n_1^2 \sin^2 \theta}}} \quad (1)$$

Received 23 October 2006; accepted 20 February 2007.

\* Author to whom correspondence should be sent. E-mail: milan@mevphotonics.com.

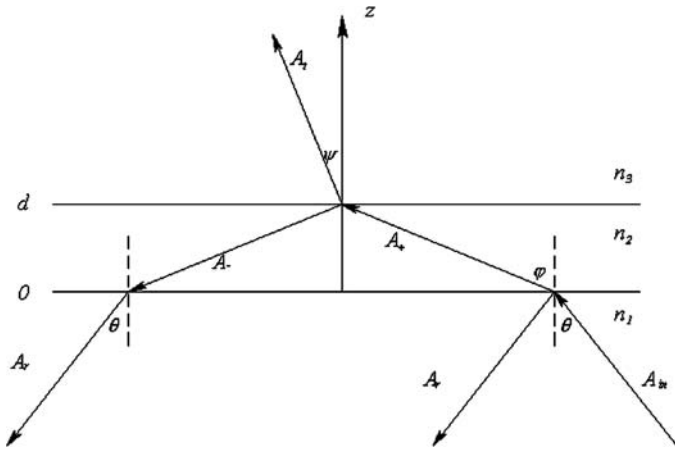


Fig. 1. Components involved in the reflection on a two-interface system.

where  $\theta$  is the angle of incidence,  $\bar{\nu}^\dagger$  is the wavenumber of incident light, and  $r_{12}^\sigma$  and  $r_{23}^\sigma$  are the Fresnel amplitude coefficients for the two polarizations  $\sigma$  ( $\sigma = s, p$ ) for the interfaces between media 1 and 2 and media 2 and 3, respectively. Equation 1 is valid even if all three media involved are absorbing, i.e., all three refractive indices are complex. In practice, the incident medium (medium 1) is always non-absorbing and hence  $n_1$  is always a real number. Medium 2 is the medium of interest (i.e., the sample), and it is generally treated as absorptive. Thus,  $n_2$  is generally a complex number. In the case of our current interest, the medium 3 could be either non-absorbing (Si substrate), hence  $n_3$  would be real, or absorbing (metal substrate), hence  $n_3$  would be complex.

Note that the reflectance coefficient (Eq. 1) for an infinitely thin film must reduce to the regular Fresnel reflectance coefficient for the interface between media 1 and 3, i.e.,  $r_{13}^\sigma$ .

The reflectance itself is the absolute value squared of Eq. 1, i.e.,

$$R^\sigma = |\rho^\sigma|^2 \quad (2)$$

The expression for thin film reflectance appears straightforward, so it should be easy to understand how the various parameters involved result in the sensitivity enhancement seen for very thin films. However, since the individual reflectance coefficients are complex numbers, the actual expression is far more complicated than it appears.

For a very thin film, the film thickness  $d$  is much smaller than the wavelength of incident light and we can expand the exponential term of Eq. 1 and rearrange it to make the expression under the square root positive:

$$e^{4\pi\bar{\nu}d\sqrt{n_2^2 - n_1^2\sin^2\theta}} \cong 1 - 4\pi\bar{\nu}d\sqrt{n_1^2\sin^2\theta - n_2^2} \quad (3)$$

Utilizing Eq. 3 in Eq. 1 yields a simplified version of Eq. 1 valid for very thin films, which, omitting polarization index for simplicity, becomes:

$$\rho \cong r_{13} \left[ 1 - 4\pi\bar{\nu}d\sqrt{n_1^2\sin^2\theta - n_2^2} \frac{r_{23}(1 - r_{12}r_{13})}{r_{12} + r_{23}} \right] \quad (4)$$

where  $r_{13}$  is the standard Fresnel amplitude coefficient for the

<sup>†</sup> Physics textbooks that cover this material use notation  $k$  for wavenumber. We follow the common practice in spectroscopy and use  $\bar{\nu}$  instead.

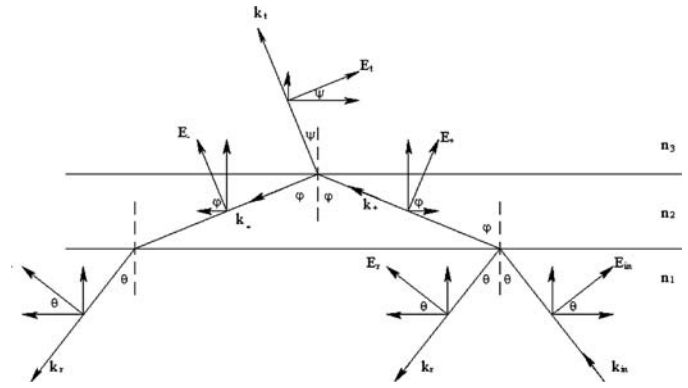


Fig. 2. Geometry of fields for a two-interface reflection system.

interface between media 1 and 3. Note that Eq. 4 explicitly becomes  $r_{13}$  in the limit where the film thickness  $d$  vanishes. The actual reflectance is the absolute value squared of the corresponding amplitude coefficient. If  $r_{13}$  is the supercritical reflectance amplitude coefficient, i.e., the amplitude coefficient where the angle of incidence is above the critical angle for total internal reflection, its absolute value is one. Thus, the GAATR reflectance for a thin film is:

$$R = |\rho|^2 \cong 1 - 8\pi\bar{\nu}d\text{Re} \left[ \sqrt{n_1^2\sin^2\theta - n_2^2} \frac{r_{23}(1 - r_{12}r_{13})}{r_{12} + r_{23}} \right] \quad (5)$$

For very thin films, the absorption is proportional to the film thickness  $d$ . The proportionality factor has the term  $r_{12} + r_{23}$  in the denominator. Hence, if an experimental configuration arises in which the two coefficients are of opposite signs and close in magnitude, the denominator becomes very small. This would greatly enhance the observed absorbance. Notice that since  $r_{12} = -r_{21}$  (see, i.e., Ref. 5), the denominator would be exactly zero if medium 3 has the same refractive index as medium 1. This, of course, would eliminate total internal reflection. It would, however, appear that if  $n_3$  is just slightly less than  $n_1$  to preserve total internal reflection,  $r_{23}$  should be close to  $r_{21}$ . Thus, when germanium is medium 1 and silicon is medium 3 for an angle of incidence above  $58.7^\circ$  (to preserve total internal reflection), the reflectance (Eq. 5) would be expected to exhibit very high sensitivity to thin films. We will return to this point when we consider specific cases later on.

The meaning of  $r_{12}$  is straightforward. It is the standard reflectance amplitude coefficient for supercritical internal reflection. However, the meaning of  $r_{23}$  is somewhat less intuitive. This is the reflectance amplitude coefficient for the interface between the film and the substrate (metal or silicon). However, since the reflection at the first interface is supercritical, the electromagnetic wave is evanescent inside the film. This means that it propagates parallel to the interfaces rather than towards the second interface. If the evanescent wave does not travel towards the second interface, it cannot reflect from it. Obviously, our intuitive notion of the reflectance coefficient fails under these conditions. Mathematically, the coefficient is still well defined since it is given as the ratio of the electric fields from the two sides of the interface. The electromagnetic wave is evanescent in the film as well as in the substrate, making the second interface an interface between two evanescent fields. Evanescent waves propagate parallel to that interface on both sides. The reflectance of that interface

can be calculated from Eq. 5, but the meaning of reflectance in this case is far from intuitive.

Perhaps we can elaborate on the meaning of Eq. 5 by comparing it to the expression for transmission through the same film. Using the thin film approximation, Lambert's law becomes:

$$T = 1 - (\log e) \cdot 4\pi\bar{v}d\kappa \quad (6)$$

where  $\kappa$ , the imaginary part of  $n_2$ , is the absorption index of the film. Note that, although formally similar, the two expressions in Eqs. 5 and 6 differ in that Eq. 5 does not exhibit the explicit dependence on  $\kappa$  as Eq. 6 does. Moreover, Eq. 6 shows explicitly that transmittance becomes zero in the absence of absorption ( $\kappa = 0$ ). It is less clear from Eq. 5 what happens in the absence of absorption. Given its physical meaning, it is obvious that in the absence of absorption, the reflectance (Eq. 5) has to become total ( $R = 1$ ). Thus, the argument of the function  $Re$  must be totally imaginary if  $\kappa = 0$ . This means that the real part of the argument of the  $Re$  function must have a real component proportional to  $\kappa$ .

**Electric Fields Inside the Film.** To more closely examine the electric fields in the film, consider the case where the angle of incidence  $\theta$  is below the critical, as shown in Fig. 2, and there is transmitted light in medium 3.

As in Fig. 1, there are two components of radiation propagating inside the film, indicated by the subscripts + and -. The orientation of the electric fields shown in Fig. 2 is that for parallel or  $p$ -polarized incident light. We can choose the coordinate system such that the  $x$ -axis is in the plane of the figure and pointing to the right along the interface between media 1 and 2, the  $z$ -axis points straight up perpendicular to the interfaces and the  $y$ -axis is pointed inward into the plane of the figure. A similar geometry holds for  $s$ -polarized incident light, but all the electric fields are along the  $y$ -axis.

From the definition of the reflectance amplitude coefficient (Eq. 1), it follows that:

$$E_r^\sigma = \rho^\sigma E_{in}^\sigma \quad (7)$$

For simplicity, we again drop the polarization index in what follows. In Fig. 2, at the interface 1, the two components of the electric field within the film are

$$E_x = (E_+ - E_-)\cos\varphi \quad (8a)$$

$$E_z = (E_+ + E_-)\sin\varphi \quad (8b)$$

The fields inside the film can be expressed in terms of the incident field. At the first interface, we have  $E_{in}$  and  $E_r$  in the first medium and  $E_+$  and  $E_-$  in the second medium.  $E_+$  contains contributions from the transmitted component of the incident field and also from the reflected component of  $E_-$ :

$$E_+ = t_{12}E_{in} + r_{21}E_- \quad (9)$$

Similarly:

$$E_r = t_{21}E_- + r_{12}E_{in} \quad (10)$$

Equations 9 and 10 can be solved for  $E_\pm$  in terms of  $E_{in}$ :

$$E_- = \frac{\rho - r_{12}}{t_{21}} E_{in} \quad (11a)$$

$$E_+ = \frac{1 - \rho r_{12}}{t_{21}} E_{in} \quad (11b)$$

These are the internal fields at the first interface ( $z = 0$ ). The two components,  $E_+$  and  $E_-$ , have different  $z$  dependences.<sup>10</sup> Thus, Eqs. 8a and 8b can be rewritten as:

$$E_x = \left\{ [(1 - \rho r_{12})e^{2\pi i\bar{v}z\sqrt{n_2^2 - n_1^2\sin^2\theta}} - (\rho - r_{12})e^{-2\pi i\bar{v}z\sqrt{n_2^2 - n_1^2\sin^2\theta}}] / (n_2 t_{21}) \right\} E_{in} \sqrt{n_2^2 - n_1^2\sin^2\theta} \quad (12a)$$

$$E_z = \left\{ [(1 - \rho r_{12})e^{2\pi i\bar{v}z\sqrt{n_2^2 - n_1^2\sin^2\theta}} + (\rho - r_{12})e^{-2\pi i\bar{v}z\sqrt{n_2^2 - n_1^2\sin^2\theta}}] / (n_2 t_{21}) \right\} n_1 E_{in} \sin\theta \quad (12b)$$

Equations 12a and 12b hold only for  $p$ -polarized light.

For  $s$ -polarized light, all the electric fields are perpendicular to the plane of incidence and hence mutually parallel. Thus, for the  $s$ -polarized beam, the equivalent of Eq. 8 is:

$$E_y = E_+ + E_- \quad (13)$$

The electric field inside the film is along the  $y$ -axis. With the help of Eqs. 11a and 11b, and keeping in mind the different  $z$  dependence of the two components, Eq. 13 becomes:

$$E_y = \left\{ [(1 - \rho r_{12})e^{2\pi i\bar{v}z\sqrt{n_2^2 - n_1^2\sin^2\theta}} + (\rho - r_{12})e^{-2\pi i\bar{v}z\sqrt{n_2^2 - n_1^2\sin^2\theta}}] / (t_{21}) \right\} E_{in} \quad (14)$$

Equations 12 and 14 give the expressions for the electric field inside the film. The electric field inside the film has different strengths in different directions.

As noticed before, this electric field can only excite the components of the molecular electric dipoles along the field. Since the absorption of light is proportional to the intensity of radiation, and the intensity is proportional to the square of the electric field, the strength of the electric field along a particular direction and the orientation of molecular dipoles along that direction determine the strength of absorbance "seen" in the reflected light.

We can define:

$$p_x = \left| \frac{E_x}{E_{in}} \right| \quad (15a)$$

$$p_y = \left| \frac{E_y}{E_{in}} \right| \quad (15b)$$

$$p_z = \left| \frac{E_z}{E_{in}} \right| \quad (15c)$$

where the  $p$ -factors indicate the relative strength of the excited field in the particular direction in the film compared to the field of the incident wave. The absolute values are used here because the ratios of the field amplitudes are complex numbers that include information about the relative phases of the fields, and these phases are not important to the absorption process. As the field strength in a particular direction increases, the absorption of light by bonds with a dipole moment component in that direction also increases. Since the absorption is proportional to

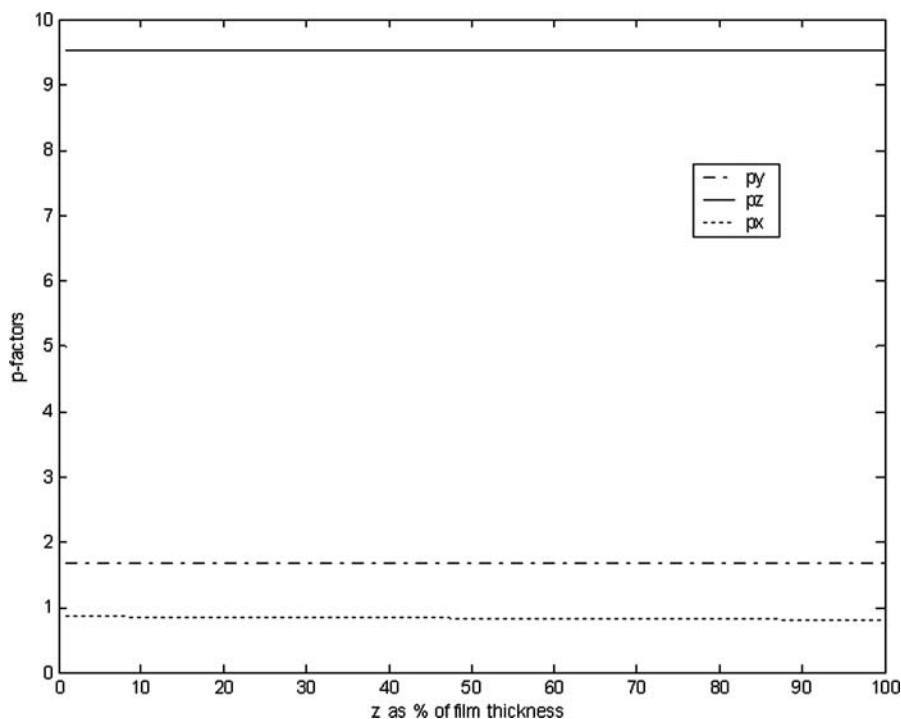


FIG. 3.  $P$ -factors versus depth  $z$  into the sample for a 10 Å thick film.

the light intensity determined by the square of the field, the square of the  $p$ -factor actually indicates the strength of absorption. Note that  $p_x$ ,  $p_y$ , and  $p_z$  are functions of  $z$ , i.e., they change with the depth into the film.

Although it is possible to obtain explicit expressions for Eqs. 15a–15c, they are too long and complicated to be informative. Therefore, the best strategy for analyzing these expressions is numerical.

## EXPERIMENTAL

The case of specific interest here is that of the GAATR technique. The experimental parameters involved are the refractive indices of the ATR crystal  $n_1$ , the substrate  $n_3$ , and the film  $n_2$ ; the thickness of the film  $d$ ; and the angle of incidence  $\theta$ .

Since most of the GAATR studies are done in the mid-infrared, we can choose the wavelength  $\lambda$  of light to be 10  $\mu\text{m}$  ( $1000\text{ cm}^{-1}$ ), in the fingerprint region. The ATR crystal is germanium with a refractive index  $n_1 = 4$  and the substrates are typically either silicon, where  $n_3 = 3.45$ , or a metal, where a typical choice of refractive index could be  $n_3 = 10 + 20i$ .

The sample should have a complex refractive index since we are interested in the supercritical regime of internal reflection for very thin absorbing films. A representative choice is  $n_2 = 1.5 + 0.1i$ . The value chosen for the absorption index  $\kappa$  ( $= 0.1$ ) corresponds to a relatively strong absorption band. Although we will vary the film thickness to explore its effect on reflectance, a good starting choice would be  $d = 10\text{ Å}$ .

We select the angle of incidence to be  $\theta = 65^\circ$ . This angle is supercritical for the Ge–Si interface and thus the electromagnetic wave above the Ge–sample interface is evanescent. Note that if we chose the incident angle to be lower, i.e.,  $45^\circ$ , the angle would still be supercritical for the Ge–sample interface and the electromagnetic wave within the film would still be

evanescent. But then the incident angle would be subcritical for the Ge–Si interface and the electromagnetic wave in silicon would be a regularly transmitted (refracted) wave with the angle of refraction determined by Snell’s law. The reflectance in this case would not be total, since some light would transmit into silicon. This ‘jumping’ of light through the film into the medium beyond is called tunneling, and it is only appreciable if the film thickness is much less than the wavelength of light.

## RESULTS AND DISCUSSION

Having decided upon a numeric approach to develop a more complete understanding of the enhancement, let us begin by examining Eq. 5. Calculating the argument of the  $Re$  function in Eq. 5 for our set of parameters with  $\kappa = 0$  gives  $55.52i$ , a huge but purely imaginary value. So  $Re$  returns zero and the reflection is total ( $R = 1$ ), as it should be. Note that the absolute value of the argument of the  $Re$  function is large. As expected, if  $r_{12} + r_{23}$  is a very small number, the absorption term is significantly enhanced. For our set of parameters,  $r_{12} + r_{23} = -0.1029 - 0.1331i$ . The vanishing of absorbance is brought about by a tenuous arrangement that keeps the large argument of the  $Re$  function purely imaginary. The delicate balance of parameters that keeps the absorption zero for  $\kappa = 0$  breaks down as soon as  $\kappa$  is no longer zero. The magnitude of the argument of the  $Re$  function is critical in the absorption enhancement for non-zero  $\kappa$ .

The magnitude of the  $Re$  function essentially originates from the strengths of the electromagnetic waves within the sample. So let us examine more closely the  $p$ -factors (Eq. 15), the relative strengths of the electric fields within the film. We can numerically calculate the  $p$ -factors in Eq. 15 as functions of the depth  $z$  into the film. Since the thickness of the sample is much less than the wavelength of the incident infrared beam, the

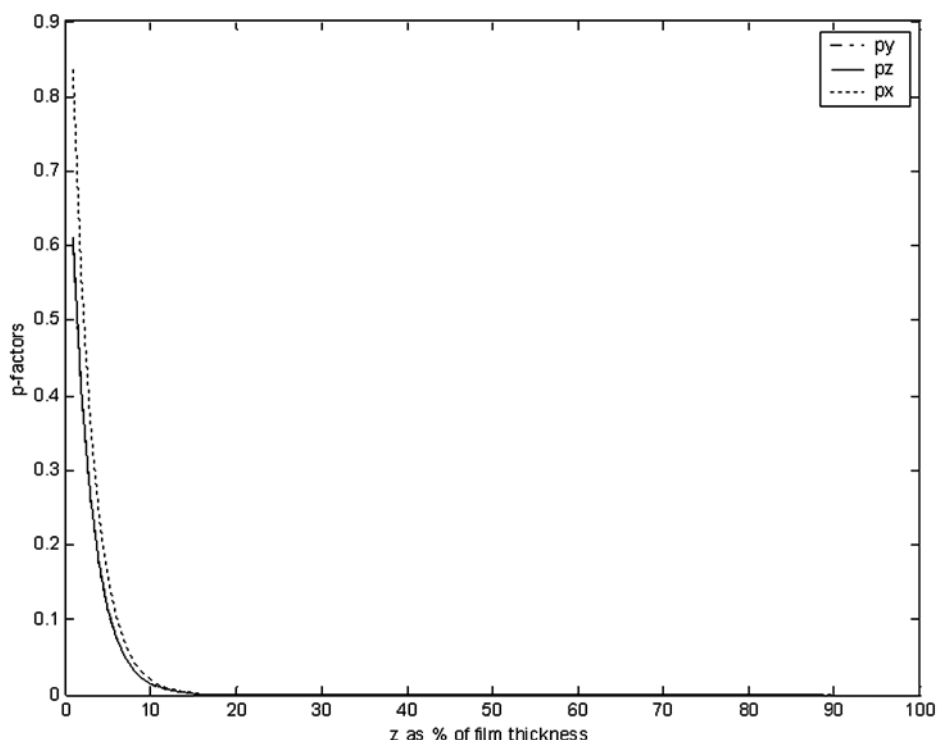


FIG. 4.  $P$ -factors versus depth  $z$  into the sample for a 10  $\mu\text{m}$  thick film.

variation of the  $p$ -factors with  $z$  is negligible. Figure 3 illustrates this situation.

The strongest field is clearly along the  $z$ -axis, i.e. perpendicular to the reflecting interfaces. Keep in mind that it is really the square of the  $p$ -factor that is important. So the field intensity along the  $z$ -direction is almost 100 times larger than the field intensity of the incident light. Recall that the coordinates were chosen so that  $p_z$  and  $p_x$  are associated with  $p$ -polarized light, while  $p_y$  is associated with  $s$ -polarized incident light. Thus we can also conclude that the absorption of  $s$ -polarized light is considerably weaker than the absorption of  $p$ -polarized light for a very thin film on the silicon substrate. Also, the absorption of  $p$ -polarized light is dominated by the absorption processes associated with the bonds whose dipole moments are aligned with  $z$ -axis, i.e., perpendicular to the interface.

It is instructive to compare the above result obtained for an ultra thin film to the analogous result for a much thicker film. A good comparison would be with a 10  $\mu\text{m}$  thick film of the same material (Fig. 4).

The exponential decrease of the fields is expected for the evanescent wave. Note that the penetration depth of the evanescent wave into the film is about 10% of the film thickness, i.e., about 1  $\mu\text{m}$ . In this case, anything much further than several micrometers beyond the first reflecting interface is irrelevant to the reflection process. The film could have been 8  $\mu\text{m}$  or 20  $\mu\text{m}$  thick, backed by silicon or anything else. The reflectance would remain unchanged since the fields vanish before reaching the substrate. Also, note that  $p_y$ , associated with the  $s$ -polarized incident light, is no longer significantly weaker as it was for the ultra thin film. But most importantly, the values of  $p_z(0)$  and  $p_x(0)$  are indicative of the remarkable enhancement in sensitivity that the GAATR technique exhibits for ultra thin films. The high

refractive index of silicon is crucial to this enhancement. If the silicon in the above ultra thin film case is replaced by glass ( $n_3 = 1.5$ ), the enhancement vanishes and the values of the  $p$ -factors resemble the above thick film case at  $z = 0$ .

Since one of the key ingredients to the enhancement is the ultra low thickness  $d$  of the film, it is of interest to see how the  $p$ -factors vary with film thickness. As we mentioned earlier, for very thin films, the fields, and thus the  $p$ -factors, do not vary significantly with the depth  $z$  into the film (see Fig. 3). For very thin films, the fields inside the film can be considered constant along the  $z$ -axis. Figure 5 shows how the  $p$ -factors inside the film vary with film thickness. As we can see from Fig. 5, the  $E_z$  and  $E_y$  fields quickly decay with an increase in film thickness while  $E_x$  slightly increases. Note that  $p_z$  falls to half of its initial value as the film thickness increases from zero to 0.05  $\mu\text{m}$ —a tiny fraction of the wavelength of incident light (10  $\mu\text{m}$ ).

It is important to note that the sensitivity of the  $s$ -polarized light to thin films is not suppressed. It is indeed stronger for thin films than for a very thick film (Fig. 4). It is the sensitivity for the  $p$ -polarized light that is remarkably enhanced. This sensitivity enhancement is due to the enhancement of the electric field component perpendicular to the interface and is thus observed only for the  $p$ -polarized incident light.

Another interesting result of the above numerical analysis is that  $p_x$ , the factor for the field component of the  $p$ -polarized light parallel to the reflecting interface, is growing with depth into the film. This differs from the behavior of the field component  $p_y$ , which, like  $p_z$ , decreases with depth into the film. Both the  $x$  and  $y$  components of the electric field are parallel to the reflecting interface and one would expect them to be affected similarly. As shown in Fig. 5 the two fields are different although both are dwarfed by the  $z$ -component.

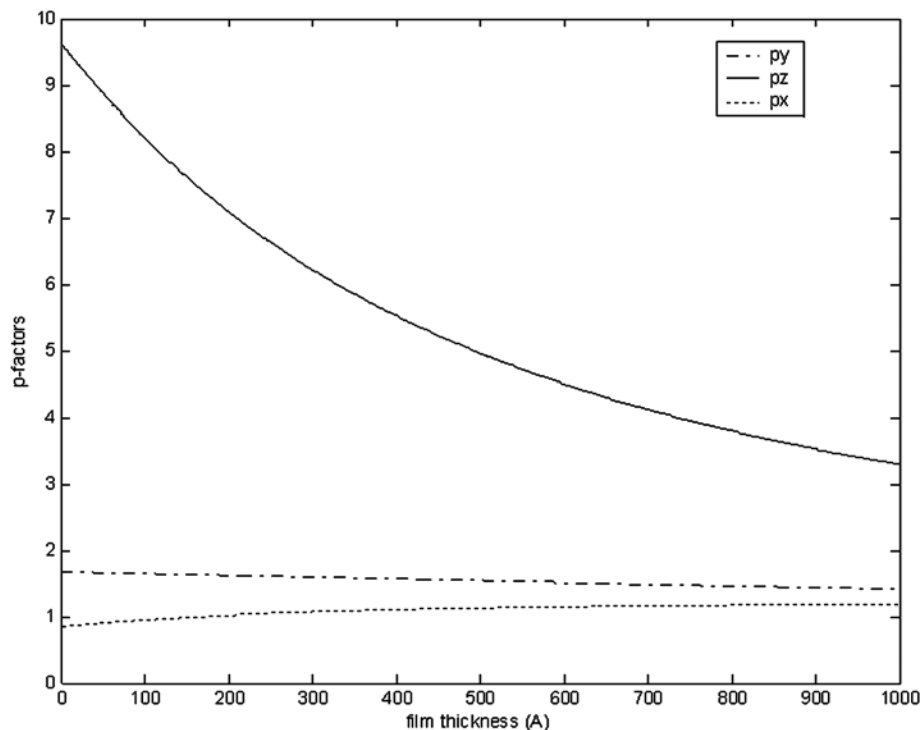


FIG. 5. *P*-factors versus film thickness for silicon substrate.

This asymmetric strength of the  $x$  and  $z$  components of the electric field inside the film could be used to an advantage. Because the perpendicular component  $E_z$  is greatly enhanced and the parallel component  $E_x$  is not, the  $p$ -polarized light essentially interacts only with dipoles perpendicular to the reflecting interface. On the other hand, the  $s$ -polarized light

interacts only with dipoles parallel to the interface. By using polarized incident light, the film can be preferentially probed in different directions to extract information on molecular orientation within the film.

Having thus far focused on a silicon substrate, let us now examine the case of a metal substrate. The case of metal

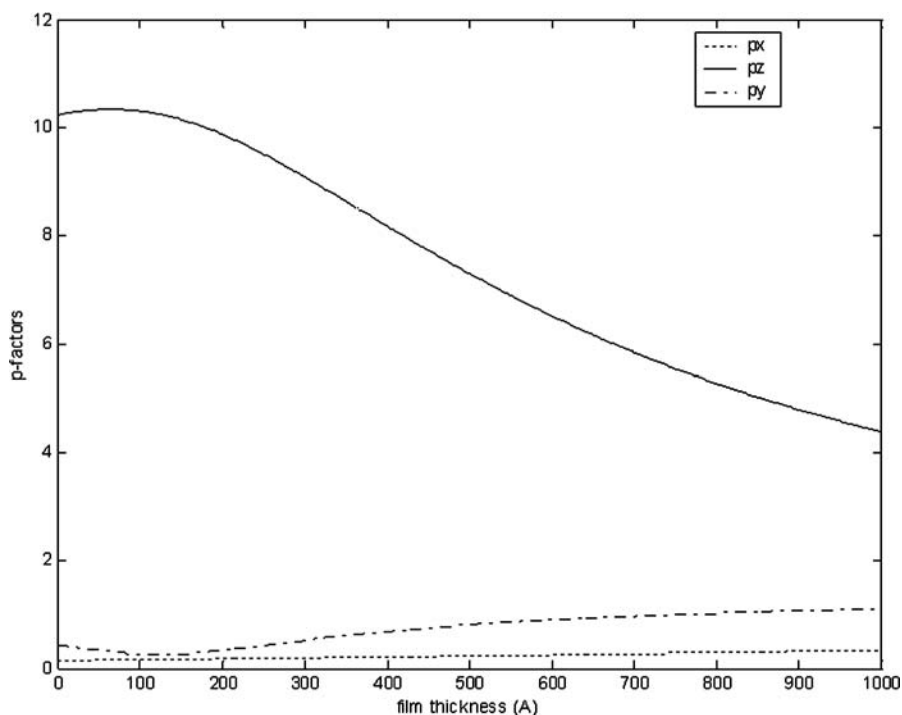


FIG. 6. *P*-factors versus film thickness for metal substrate.

substrate is interesting because the results resemble those obtained with the silicon substrate even though the reflectance is not technically internal. All the theoretical results obtained with the silicon substrate (Eqs. 12 and 14) are formally applicable to the case of a metal substrate if an appropriate choice of the refractive index of the substrate  $n_3$  is made. Selecting  $n_3 = 10 + 20i$  for a typical metal substrate gives the results in Fig. 6, showing the variation of the  $p$ -factors inside the film as a function of film thickness. Note that the electric field component  $E_z$  perpendicular to the interfaces reaches a maximum for films around 70 Å thick. The component  $E_x$  parallel to the interfaces reaches a minimum for a film thickness around 140 Å. Also,  $E_y$  is now weaker than  $E_x$ . However,  $E_z$  achieves similar strengths as it does for the case of the silicon substrate. Interestingly, although the refractive index of metal is nothing like that of silicon, and our argument about  $r_{23}$  being close to  $-r_{12}$  cannot be applied in the case of metal, it still turns out that  $r_{12} + r_{23} = 0.0816 - 0.1016i$ , a small number explaining the strong boost in sensitivity observed with metal substrates for the  $p$ -polarized incident light.

## CONCLUSION

In conclusion, the electric field strength enhancement within the sample for GAATR is highly dependent on the direction of the field. The field perpendicular to the interface is greatly enhanced. Since only  $p$ -polarized light has a component of electric field perpendicular to the interface, the sensitivity enhancement is confined to  $p$ -polarized light. As a result, only the bonds whose dipole moments have components perpendicular to the interface contribute significantly to the measured absorbance. If the bonds have dipole moments parallel to the interface, the absorption due to those bands essentially remains unobserved with  $p$ -polarized light. The absorbances of the bonds whose dipole moments are perpendicular to the interface, however, are intensely enhanced. The enhancement is roughly 100 times what the same film would absorb in transmittance. The bonds whose dipole moments are parallel to the interface are invisible to  $p$ -polarized light since they are overwhelmed by the absorbance due to perpendicular dipoles.

However, for  $s$ -polarized light, only the bonds parallel to the interface contribute. Although the absorbance due to parallel bonds is only mildly enhanced, it is not overwhelmed by the contribution due to perpendicular bonds, and although very weak, the absorbance features can be observed. Thus, if the thin film exhibits a degree of molecular orientation, the orientation information can be extracted from spectra by comparing the results obtained for the two polarizations. Although molecular orientation information can be obtained from polarized spectra in standard ATR, the information on the perpendicular bonds is always mixed with the information on the parallel bonds. One has to record ATR spectra with  $p$ -polarized light at two different incident angles and then separate the contributions of the differently oriented bonds. This can be done because the relative contributions of the two bond orientations change for different angles of incidence. However, the angle of incidence in spectroscopy is only the nominal angle. There is always a substantial spread of rays around the nominal angle, so the angular information is never clearly resolved.

Thus, GAATR spectroscopy not only provides enhanced sensitivity for examining ultra thin films on high refractive index substrates such as polished metals and silicon, but it also cleanly and explicitly separates the contributions from differently oriented bonds.

- 
1. N. J. Harrick and F. K. DuPre, *Appl. Opt.* **5**, 1739 (1966).
  2. J. E. Olsen and F. Shimura, *Appl. Phys. Lett.* **53**, 1934 (1988).
  3. J. E. Olsen and F. Shimura, *J. Appl. Phys.* **66**, 1353 (1989).
  4. M. Milosevic, S. L. Berets, and A. Y. Fadeev, *Appl. Spectrosc.* **57**, 724 (2003).
  5. N. Rochat, et al., *Mater. Sci. Eng. B* **102**, 16 (2003).
  6. M. E. Mulcahy, S. L. Berets, M. Milosevic, and J. Michl, *J. Phys. Chem. B* **108**, 1519 (2004).
  7. T. Lummerstorfer and H. Hoffman, *Langmuir* **20**, 6542 (2004).
  8. T. Lummerstorfer, C. Sohar, G. Fiedbacher, and H. Hoffman, *Langmuir* **22**, 18 (2006).
  9. M. D. Rowe-Konopacki and S. G. Boyes, *Macromolecules*, paper in press (2007).
  10. M. Milosevic and S. L. Berets, *Appl. Spectrosc.* **47**, 5666 (1993).